AGU PUBLICATIONS

Geophysical Research Letters

RESEARCH LETTER
10.1002/2017GL075052

**Key Points:**
- Seasonal forecasts of California precipitation have performed poorly during the last two winters
- Subseasonal forecasts skillfully predicted monthly precipitation anomalies in California during January and February of 2016 and 2017
- California precipitation anomalies are associated with predictable shifts in the position of the jet stream over the northeast Pacific

**Supporting Information:**
- Supporting Information S1

**Correspondence to:**
S. Wang,
sw2526@columbia.edu

**Citation:**
Wang, S., Anichowski, A., Tippett, M. K., & Sobel, A. H. (2017). Seasonal noise versus subseasonal signal: Forecasts of California precipitation during the unusual winters of 2015–2016 and 2016–2017. *Geophysical Research Letters*, *44*, 9513–9520. https://doi.org/10.1002/2017GL075052

Received 23 JUL 2017
Accepted 12 SEP 2017
Accepted article online 18 SEP 2017
Published online 30 SEP 2017



# Seasonal Noise Versus Subseasonal Signal: Forecasts of California Precipitation During the Unusual Winters of 2015–2016 and 2016–2017

**Shuguang Wang[1], Alek Anichowski[1], Michael K. Tippett[1,3], and Adam H. Sobel[1,2]**

[1]Department of Applied Physics and Applied Mathematics, Columbia University, New York, NY, USA, [2]Lamont-Doherty Earth Observatory, Columbia University, Palisades, NY, USA, [3]Department of Meteorology, Center of Excellence for Climate Change Research, King Abdulaziz University, Jeddah, Saudi Arabia

**Abstract** Subseasonal forecasts of California precipitation during the unusual winters of 2015–2016 and 2016–2017 are examined in this study. It is shown that two different ensemble forecast systems were able to predict monthly precipitation anomalies in California during these periods with some skill in forecasts initialized near or at the start of the month. The unexpected anomalies in February 2016, as well as in January and February 2017, were associated with shifts in the position of the jet stream over the northeast Pacific in a manner broadly consistent with associations found in larger ensembles of forecasts. These results support the broader notion that what is unpredictable atmospheric noise at the seasonal time scale can become predictable signal at the subseasonal time scale, despite that the lead times and verification averaging times associated with these forecasts are outside the predictability horizons of canonical midrange weather forecasting.

## 1. Introduction

Prolonged severe drought in California from 2011 to 2016 placed great stress on the state's water resources. Onset of the strong warm El Niño–Southern Oscillation (ENSO) event in the central and eastern Pacific Ocean in the summer and fall of 2015, with tropical Pacific sea surface temperature (SST) anomalies exceeding even those of the extreme 1997–1998 event, was widely expected to bring much-needed rain to California as the winter rainy season approached (e.g., Hoell et al., 2016; Steinschneider and Lall, 2016), raising hopes that the drought would be alleviated. Seasonal forecast systems—for example, those participating in the North American Multi-Model Ensemble (NMME) project (Cohen et al., 2017; Kirtman et al., 2014; Wanders et al., 2017)—consistently predicted, in forecasts initialized during the fall and early winter, that the winter as a whole would be anomalously wet. To the contrary, however, anomalously dry conditions were observed in midwinter, and particularly in February, despite the continued presence of strong warm SST anomalies in the eastern Pacific (Figure 1). Similar seasonal forecast failures, though of the opposite sign, occurred during the following winter, 2016–2017. Despite the occurrence of a weak La Niña event during the winter 2016–2017, this rainy season became the second wettest in the 122 years of record.

It can be argued that despite appearances, the seasonal forecast systems were not necessarily wrong, if interpreted probabilistically. Kumar and Chen (2016) find that the observed California precipitation anomalies during the winter of 2015–2016 (overlapping 3 month seasons from November 2015 through February 2016) were, despite being much drier than the ensemble mean, still well within the distribution of seasonal precipitation anomalies predicted by a large seasonal forecast model ensembles under strong ENSO conditions. An appropriate probabilistic forecast based on such ensembles may be viewed as a superposition of predictable seasonal component and weather "noise" that is defined as such by being unpredictable at the lead time of interest. That noise component just happened to dominate the predictable seasonal signal in the last two winters. Cohen et al. (2017) note in addition that observed precipitation amounts for Seattle and Los Angeles were outside the range of the NMME ensemble predictions for DJF (December–February) 2015–2016, suggesting that these models may underestimate noise or miss predictable seasonal components attributable to certain remote large-scale influences on California precipitation (Mo and Higgins, 1998; Hartmann, 2015; Hoell et al., 2016; Seager and Henderson, 2016; Cohen, 2016; Swain et al., 2016; Teng & Branstator, 2017; Paek et al., 2017; Wang et al., 2014).

What is unpredictable at the seasonal time scale, in any case, can become predictable at the subseasonal time scale. In this study, we show that current subseasonal prediction systems were able to predict monthly

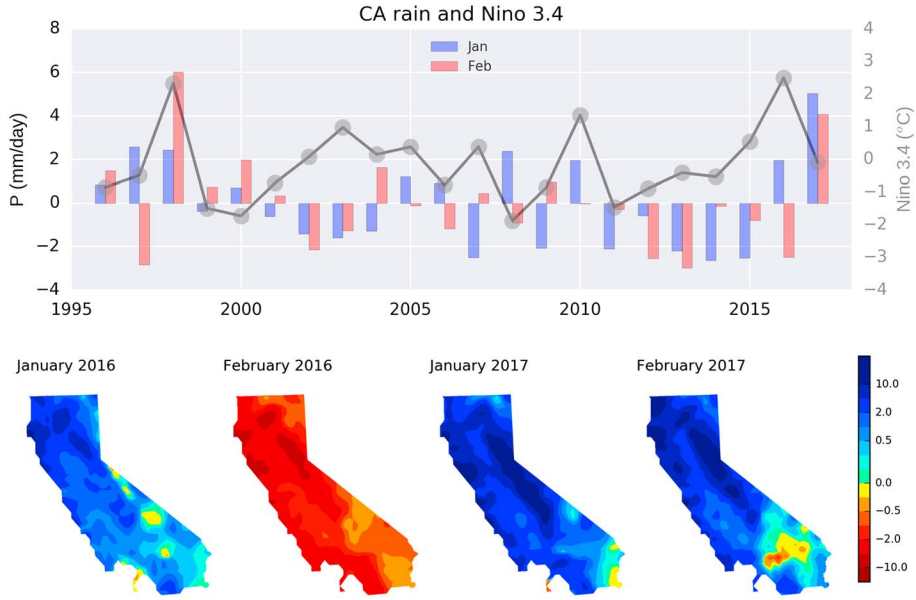


**Figure 1.** (top) Observed Niño 3.4 index (degrees) averaged over January and February since 1995 and observed precipitation anomalies (mm/d) averaged separately over January (red) and February (blue) since 1997 from CPC. (bottom) Precipitation anomalies (mm/d) over California in January and February 2016 and 2017.

precipitation anomalies in California during January and February of 2016 and 2017 with some skill in forecasts initialized near or at the start of the month. The unexpected anomalies in February 2016 and in January and February 2017 were associated with shifts in the position of the jet stream over the northeast Pacific in a manner broadly consistent with associations found in larger ensembles of forecasts. Noise in the seasonal forecasts became signal in the subseasonal forecasts. Better understanding of this transition, as both forecast lead time and the averaging time for verification (e.g., Wheeler et al., 2016; Zhu et al., 2014) decrease from several months to several weeks, could allow subseasonal forecasts to become more widely used and their value to increase.

## 2. Data

Real-time forecasts from the European Centre for Medium-Range Weather Forecasting (ECMWF) and the U.S. National Center for Environmental Prediction (NCEP) were obtained from the World Meteorological Organization (WMO) Subseasonal-to-seasonal (S2S) Prediction Project database (Vitart et al., 2017). Forecast precipitation anomalies are calibrated with reforecast data by subtracting the reforecast climatology from the real-time forecast computed as a function of both lead time and initialization date. The ECMWF and NCEP Climate Forecast System version (CFSv2) systems are integrated for similar lead times (47 days and 46 days, respectively) for subseasonal prediction, but the two employ different ensemble initialization strategies: the ECMWF system initializes real-time forecasts every Monday and Thursday with 51 ensemble members initialized simultaneously, and its 10-member ensemble reforecast is initialized at the same calendar date of the last 20 years (i.e., the on-the-fly method). The CFSv2 system initializes real-time forecasts every day with 16 lagged (four every 6 h) ensemble members, and its four-member ensemble reforecast is produced each day from 1999 to 2011 (i.e., the fixed method). In addition to the S2S data, the CFSv2 seasonal forecasts and hindcasts (Saha et al., 2014) are used to explore to study the dependence of the forecast on lead time.

We use the CPC 0.25 × 0.25 Daily U.S. Unified Gauge-Based Analysis of Precipitation data (Chen et al., 2008; Xie et al., 2007) to compute rain anomalies. NCEP-2 reanalysis data (Kanamitsu et al., 2002) is used to analyze atmospheric wind fields. The CPC monthly SST indices are used to represent ENSO SST (OISST v2; http://www.cpc.ncep.noaa.gov/data/indices/sstoi.indices).

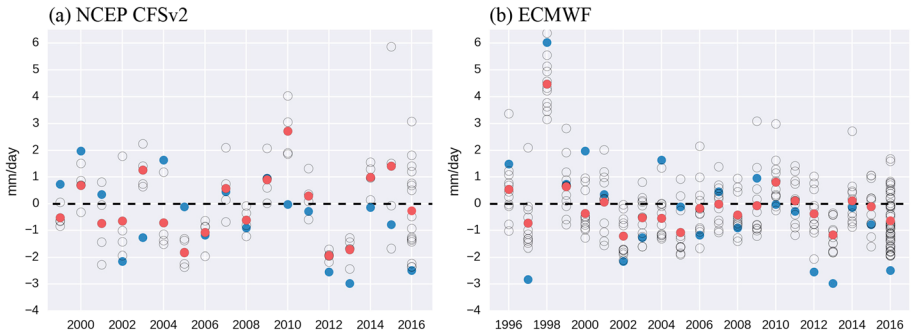


**Figure 2.** Real-time monthly prediction and reforecasts of California rain anomalies (forecasts of the monthly mean from model runs initialized on the first of the month) for February 2016 from (left) CFSv2 and (right) ECMWF. Open circles are individual ensemble members, red dots are ensemble means, and blue dots are observed anomalies.

## 3. Subseasonal Prediction of CA Precipitation

As our focus is on California monthly precipitation in January and February, Figure 1 shows these quantities from 1996 to 2017, together with the Nino3.4 index. The strong subseasonal variability in early 2016 is apparent, with the wet anomaly in January and dry anomaly in February, as well as the wet anomalies in both January and February 2017. Figure 1 (bottom) shows maps of monthly precipitation over the state.

Figure 2 shows ensemble forecasts of area-averaged February precipitation anomalies from reforecast and real-time forecasts initialized at the beginning of the month. ECMWF forecasts predicted that California would be anomalously dry in February 2016 in the ensemble mean, but only slightly in the case of the CFSv2 forecast. Ensemble member values range from −2.5 to 3 mm/d.

California ensemble-mean precipitation anomalies by all the real-time forecasts over these periods from CFSv2 and ECMWF are summarized in Figure 3 as a function of target date and lead time, in so-called chiclet diagrams (Carbin et al., 2016). CPC rain gauge precipitation data are shown at the bottom of each panel. Forecasts at very short lead times are close to observation, so that differences between values at longer lead times and those at short lead times may be interpreted to be errors in the longer-lead forecasts. Features in this chiclet diagram are typically vertically aligned at short lead times, indicating forecasts that make consistent predictions for a given verification time from one model run to the next. Such vertical alignment may be considered a pragmatic definition of predictability on these time scales.

Wet anomalies in late January 2016 were consistently predicted ~30 days ahead, far exceeding the 2 week canonical weather prediction limit (Lorenz, 1963). The dry conditions in early to mid-February (before the twentieth of the month) also began to be predicted a few weeks ahead. Wet anomalies were incorrectly predicted to occur during the last 10 days of February at lead times greater than 2 weeks but were replaced by forecasts of dry anomalies at a lead time of approximately 2 weeks.

The dependence of forecast accuracy on lead time is explored with seasonal CFSv2 forecasts, which consist of 4 of the 16 subseasonal forecasts extended out to cover the next nine calendar months (Saha et al., 2014). The longer lead times of the seasonal system allow us to study the dependence of the forecast on lead time over a wider range and to see the transition from the ENSO-forced seasonal signal to the (presumably ENSO-independent) subseasonal signal. Evaluation of the forecast skill in California monthly rain anomalies, measured by anomaly correlation between forecast and observations, indicates that the CFSv2 four-member ensemble forecast has little skill (correlation skill of ~0.3) beyond 50 days, a value that gradually increases as lead time decreases (supporting information Figure S1).

Figure 4 shows the predicted monthly rain anomalies over California for January and February of 2016 and 2017 as lead time decreases from 5 months to −5 days, where day zero is defined as the first day of the month being forecast. For January and February 2016, a persistent wet signal is seen in the forecasts with lead time greater than 30 days. For February 2016 targets, the wet signal is substantially reduced starting about 40 days out, and starts at the end of January begin to show negative anomalies. For January targets, there is little systematic change in the forecast values as lead times decrease. In all cases, forecasts initialized at and after day zero consistently predict the correct sign of the observed anomalies. This is a nontrivial

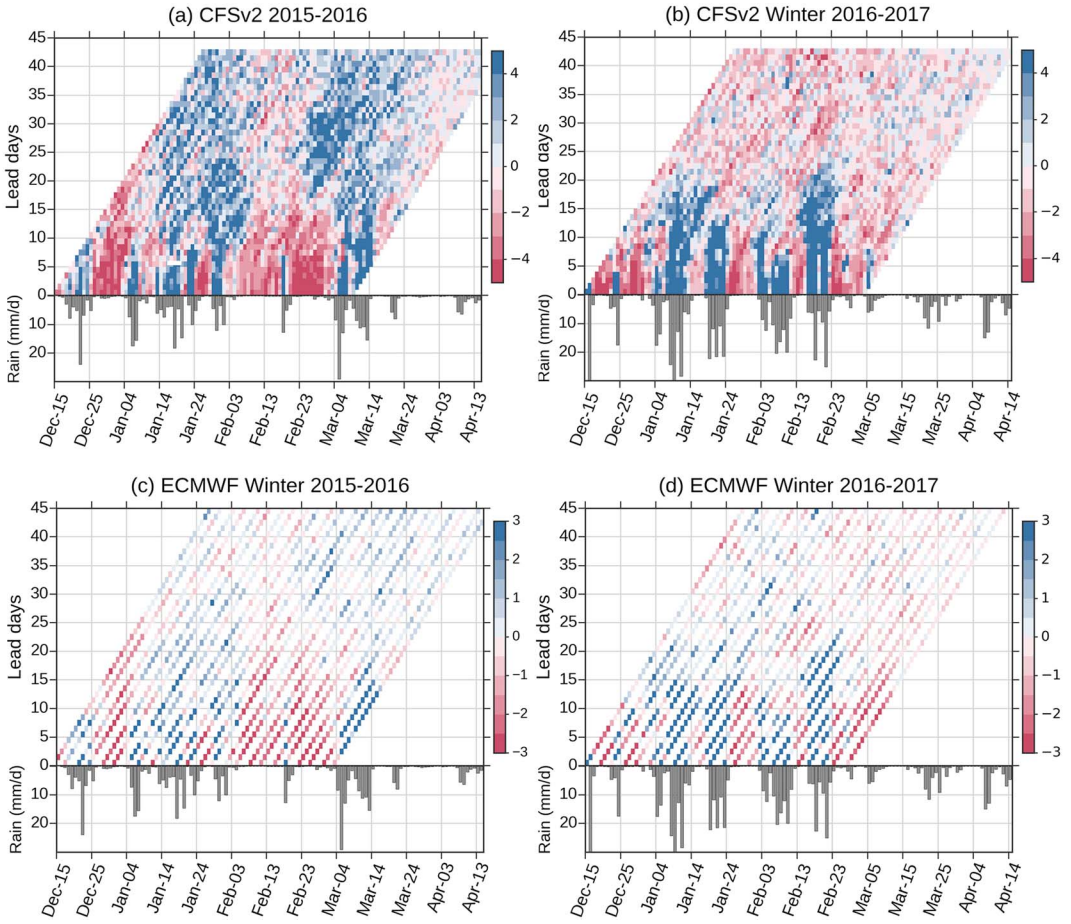


**Figure 3.** Chiclet diagram of daily California ensemble-mean precipitation anomaly forecasts from the CFSv2 for (a) 2016 and (b) 2017 and from the ECMWF S2S forecast data for (c) 2016 and (d) 2017, as a function of the verification date (horizontal axis) and lead time (vertical axis). Time series of CPC daily mean California precipitation is plotted with *y* axis inverted.

result, given that a monthly forecast initialized on day zero can be considered to have an average lead time of 2 weeks. For January and February 2017 targets, overall neutral or dry conditions were predicted at lead times greater than 20 days. At about leads of 2 weeks, a shift toward wet anomalies starts that is established (with the anomaly sign becoming positive) by day zero. Thus, similar transitions from seasonal to subseasonal signal occur in both 2016 and 2017 as the lead time is reduced from that associated with seasonal to subseasonal (in this case, monthly) forecasts. In three of the four target months, the subseasonal signal that appeared was the opposite of the seasonal one.

To understand the predictability of these precipitation anomalies at the subseasonal time scale, we examine the relationship between monthly California rainfall anomalies and zonal wind anomalies as shown in Figure 5. This pattern has a tripolar structure over the northeast Pacific with easterly anomalies in the deep tropics, westerlies centered around 30°N, and easterlies centered around 50°N. The tropical easterlies are associated with ENSO SST anomalies and are likely stationary responses to tropical heating (e.g., Trenberth et al., 1998), while the extratropical response represents a shift of a local jet. On the monthly time scale, California has positive monthly precipitation anomalies when the wind anomalies are of the sign shown, easterly in the tropics and westerly in the subtropics.

To study the implications of this wind pattern further, we construct a local index focused on the zonal wind in midlatitudes, computed as the difference between the area-averaged zonal wind anomalies in the two boxes in the northeastern Pacific shown in Figures 5a and 5b. Tropical latitudes are omitted because of their weaker correlation and presumably less direct dynamical connection to California precipitation. The linear correlation

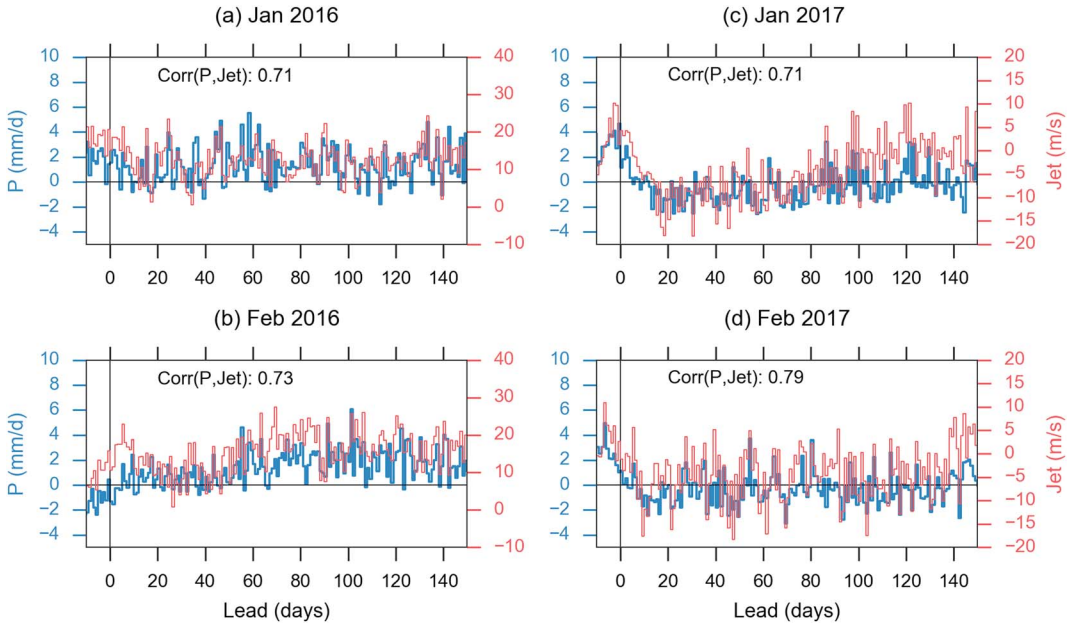


**Figure 4.** Predicted California area-averaged precipitation anomalies (blue) and the local jet index (red) predicted by the CFSv2 forecast system as a function of lead time for January and February in (a, b) 2016 and (c, d) 2017, respectively. Negative lead time indicates that the forecast initialization dates are after the start of the target month. Correlation between rain anomalies and jet index is denoted in each panel.

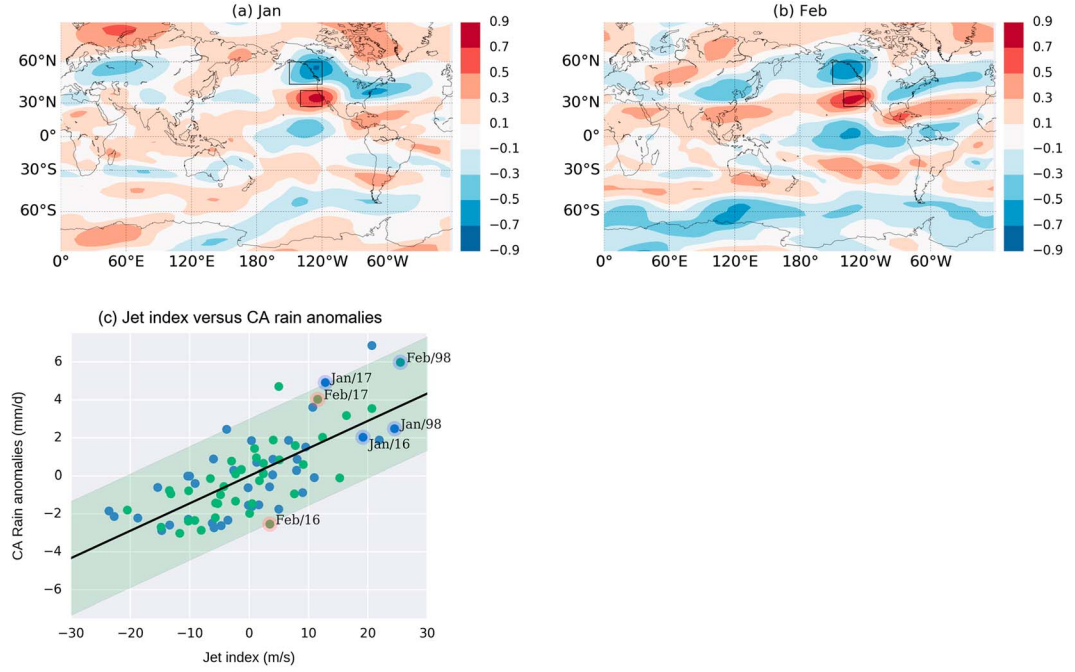


**Figure 5.** Correlation between CA precipitation anomalies and 200 monthly zonal wind anomalies in (a) January and (b) February from 1997 to 2017. (c) A local jet index and monthly CA precipitation anomaly for January (blue) and February (red) from 1979 to 2017. The jet index is computed as the difference of zonal wind at 200 hPa between two areas in northeast eastern Pacific as U200 [220–240°E, 27–40°N]–U200 [210–240°E, 45–60°N], as indicated by the two box in the Figures 5a and 5b. Correlation between the two variables is ~0.72. Explained variance by a linear fit: $P$ (mm/d) = 0.146 × Jet (m/s) is 0.52. January and February in 1998, 2016, and 2017 are labeled in Figure 5c. Shaded region indicates 2 sigma area of linear regression errors.

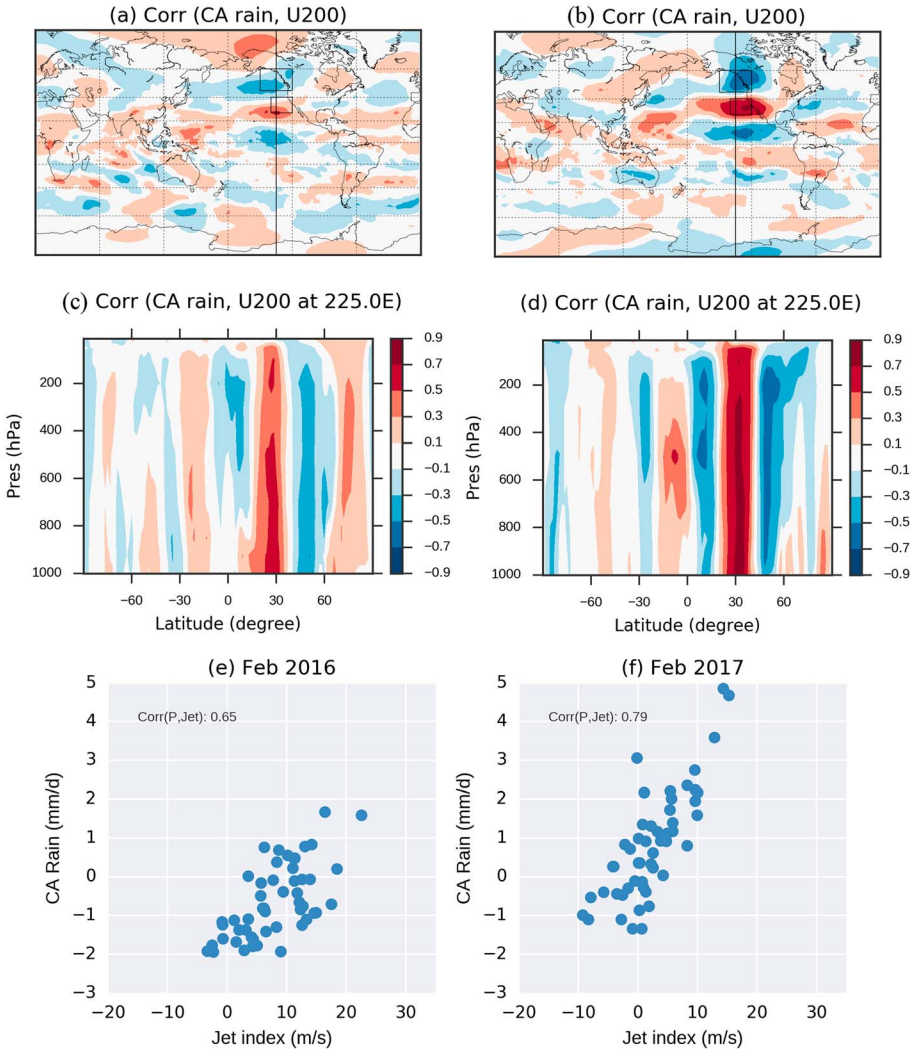


**Figure 6.** (a, c, and e) Correlation coefficient between California rain and zonal wind anomalies among 51 members of the ECMWF S2S forecast ensemble initialized on 1 February 2016, as a function of latitude and longitude at 200 hPa (Figure 6a) and as a function of pressure and latitude at 225°E (Figure 6c). Jet index (m/s) versus CA rain anomalies (mm/d) for individual ensemble members (Figure 6e). (b, d, and f) As in Figures 6a, 6c, and 6e but for the forecast ensemble initialized on 30 January 2017.

between the California rain anomalies and our local jet index is 0.72, explaining 52 percent of the variance. This local jet index is not independent of ENSO: the linear correlation coefficient between the jet index and Nino 3.4 index is 0.58, which is statistically significant at 95%, but the zonal wind index directly explains a larger fraction of monthly California rain variability than does ENSO.

Linear regression of precipitation anomalies against the observed zonal wind index indicates strong wet anomalies in both January and February 1998, when the warm ENSO event was among the strongest on record. The January and February 2017 wet anomalies can also be predicted by the linear fit qualitatively, although their values (>4 mm/d) exceed the linear regression line by 2 mm/d. In January 2016, the jet index is high, coincident with the strong wet anomaly. On the other hand, the local jet index is weakly positive or nearly neutral in February 2016, which would indicate a weak wet anomaly; but a dry anomaly with more than 2 mm/d below the linear regression were observed at CA, which lies on the 2 sigma of the linear regression error range. The difference of the zonal wind index from what would have been expected from the ENSO state alone was thus of the right sign, but not the right amplitude, to explain the dry anomalies.

The local jet index predicted by CFSv2 (red curves in Figure 4) covaries with the predicted rain anomalies at most lead times for these winter months. Both jet strength and precipitation consistently increase as lead time decreases below about 20 days in both January and February 2017. As might be expected from Figure 5, the situation is less clear for February 2016. An increase in the jet was predicted by forecasts initialized in the last 10 days of January 2016, decreasing but remaining positive in subsequent forecasts and only becoming negative in those initialized after the beginning of February.

Despite that the February 2016 CA dry anomalies are not well explained by the linear regression of the local jet index, our analysis indicates that there is nonetheless a strong relationship between forecast California precipitation anomaly and jet activity. This is examined with the ECMWF ensemble forecasts, which have a much larger ensemble size and predicted a weak dry anomaly at the beginning of February 2016. Correlation among the 51 members between predicted California rain anomaly and zonal wind index (Figure 6), without bias correction, shows a tripolar pattern similar to that in Figure 5, with vertical structure shown here to be coherently distributed from the surface to the tropopause. This pattern is similar to the wind-rain association derived from ensemble forecasts made at the end of the January 2017 (Figures 6b and 6d). The jet index and California rain, both bias corrected, are well correlated among the ensemble members (Figures 6e and 6f) in these 2 months, with a better correlation in February 2017. This is evidence that a relatively weak jet offshore of California was associated with the suppressed precipitation forecast.

## 4. Summary

Seasonal forecasts of California precipitation during the winters of 2015–2016 and 2016–2017 were unsuccessful to the extent that they did not anticipate the large observed anomalies with signs opposite to those that would have been consistent, on average, with the ENSO state. Here we have explored the predictability and prediction of these anomalies at the subseasonal time scale using forecast and reforecast data from the WMO S2S project. We show that in the monthly forecast—the forecast for the monthly mean precipitation made at the start of the month in question—the ECMWF and NCEP CFSv2 forecast models consistently predict the right sign of rainfall anomalies. At longer lead times, these models predicted anomalies consistent with the ENSO state, consistent with the argument that the observed anomalies were due to unpredictable atmospheric "noise." As the lead time reduces from seasonal to subseasonal time scales, however, noise becomes signal, and the forecasts change, achieving at least the correct sign, if not magnitude, of the precipitation anomalies eventually observed. While it is not at all surprising that forecasts become more accurate at shorter lead times, until relatively recently it would not have been plausible to expect good performance from a monthly forecast. We illustrate that the subseasonal predictability which provides the motivation and focus for the S2S project was specifically operative during these high-impact and high-visibility cases during which seasonal forecasts failed despite the presence of strong ENSO anomalies.

Analysis of the subseasonal forecast ensemble reveals that California precipitation is well correlated with zonal wind in the northeast Pacific with a tripolar structure in latitude. This consistent correlation indicates that dry anomalies in February 2016 and wet anomalies in both January and February 2017 were both associated with fluctuations in that zonal wind pattern and suggests that the dynamics and predictability of that pattern are relevant to a better understanding (and perhaps more effective practical use) of subseasonal forecasts of U.S. west coast precipitation.

This case study also illustrates the broader notion that what is unpredictable atmospheric noise at the seasonal time scale can become predictable signal at the subseasonal time scale, despite that the lead times and verification averaging times associated with subseasonal forecasts are outside the predictability horizons associated with traditional weather forecasting. State-of-the-art forecast systems are now capable of making consistent and skillful subseasonal forecasts thanks to continuous improvement in the forecast models and data assimilation techniques.

**Acknowledgments**
This research has been conducted as part of the NOAA MAPP S2S Prediction Task Force and supported by NOAA grant NA16OAR4310076. We also acknowledge support from NSF AGS-1543932. A. A. was partly supported by an NSF Research Experiences for Undergraduates (REU) supplement as part of the latter project. We thank Haibo Liu for obtaining and organizing the S2S data set from the ECMWF data portal. We are grateful to two anonymous reviewers for their constructive comments. SW thanks Xiaosong Yang for sharing his insights. The NCEP CFSv2 seasonal forecast is obtained from climate data library hosted at IRI/Columbia University. CPC U.S. Unified Precipitation data were provided by the NOAA/OAR/ESRL PSD, Boulder, Colorado, USA, from their Web site at http://www.esrl.noaa.gov/psd/.

## References

Carbin, G. W., Tippett, M. K., Lillo, S. P., & Brooks, H. E. (2016). Visualizing long-range severe thunderstorm environment guidance from CFSv2. *Bulletin of the American Meteorological Society*, *97*, 1021–1031. https://doi.org/10.1175/BAMS-D-14-00136.1

Chen, M., Shi, W., Xie, P., Silva, V. B. S., Kousky, V. E., Wayne Higgins, R., & Janowiak, J. E. (2008). Assessing objective techniques for gauge-based analyses of global daily precipitation. *Journal of Geophysical Research*, *113*, D04110. https://doi.org/10.1029/2007JD009132

Cohen, J. (2016). Weather forecasting: El Niño dons winter disguise as La Niña. *Nature*, *533*, 179.

Cohen, J., Pfeiffer, K., & Francis, J. (2017). Winter 2015/16: A turning point in ENSO-based seasonal forecasts. *Oceanography*, *30*, 82–89.
Hartmann, D. L. (2015). Pacific sea surface temperature and the winter of 2014. *Geophysical Research Letters*, *42*, 1894–1902. https://doi.org/10.1002/2015GL063083
Hoell, A., Hoerling, M., Eischeid, J., Wolter, K., Dole, R., Perlwitz, J., … Cheng, L. (2016). Does El Niño intensity matter for California precipitation?, *Geophysical Research Letters*, *43*, 819–825. https://doi.org/10.1002/2015GL067102
Kanamitsu, M., Ebisuzaki, W., Woollen, J., Yang, S., Hnilo, J. J., Fiorino, M., & Potter, G. L. (2002). NCEP–DOE AMIP-II Reanalysis (R-2). *Bulletin of the American Meteorological Society*, *83*, 1631–1643. https://doi.org/10.1175/BAMS-83-11-1631
Kirtman, B. P., Min, D., Infanti, J. M., Kinter, J. L., Paolino, D. A., Zhang, Q., … Wood, E. F. (2014). The North American multimodel ensemble: Phase-1 seasonal-to-interannual prediction: Phase-2 toward developing intraseasonal prediction. *Bulletin of the American Meteorological Society*, *95*, 585–601. https://doi.org/10.1175/BAMS-D-12-00050.1
Kumar, A., & Chen, M. (2016). What is the variability in US west coast winter precipitation during strong El Niño events? *Climate Dynamics*. https://doi.org/10.1007/s00382-016-3485-9
Lorenz, E. N. (1963). Deterministic nonperiodic flow. *Journal of the Atmospheric Sciences*, *42*, 433–471.
Mo, K. C., & Higgins, R. W. (1998). Tropical influences on California precipitation. *Journal of Climate*, *11*, 412–430. https://doi.org/10.1175/1520-0442(1998)011<0412:TIOCP>2.0.CO;2
Paek, H., Yu, J.-Y., & Qian, C. (2017). Why were the 2015/2016 and 1997/1998 extreme El Niños different? *Geophysical Research Letters*, *44*, 1848–1856. https://doi.org/10.1002/2016GL071515
Saha, S., Moorthi, S., Wu, X., Wang, J., Nadiga, S., Tripp, P., … Becker, E. (Eds.) (2014). The NCEP Climate Forecast System version 2. *Journal of Climate*, *27*, 2185–2208. https://doi.org/10.1175/JCLI-D-12-00823.1
Seager, R., & Henderson, N. (2016). On the role of tropical ocean forcing of the persistent North American west coast ridge of winter 2013/14. *Journal of Climate*, *29*, 8027–8049. https://doi.org/10.1175/JCLI-D-16-0145.1
Steinschneider, S., & Lall, U. (2016). El Niño and the U.S. precipitation and floods: What was expected for the January–March 2016 winter hydroclimate that is now unfolding? *Water Resources Research*, *52*, 1498–1501. https://doi.org/10.1002/2015WR018470
Swain, D., Horton, D., Singh, D., & Diffenbaugh, N. (2016). Trends in atmospheric patterns conducive to seasonal precipitation and temperature extremes in California. *Science Advances*, *2*, e1501344–e1501344. https://doi.org/10.1126/sciadv.1501344
Teng, H., & Branstator, G. (2017). Causes of extreme ridges that induce California droughts. *Journal of Climate*, *30*, 1477–1492. https://doi.org/10.1175/JCLI-D-16-0524.1
Trenberth, K. E., Branstator, G. W., Karoly, D., Kumar, A., Lau, N.-C., & Ropelewski, C. (1998). Progress during TOGA in understanding and modeling global teleconnections associated with tropical sea surface temperatures. *Journal of Geophysical Research*, *103*, 14,291–14,324. https://doi.org/10.1029/97JC01444
Vitart, F., Ardilouze, C., Bonet, A., Brookshaw, A., Chen, M., Codorean, C., … Zhang, L. (2017). The subseasonal to seasonal (S2S) prediction project database. *Bulletin of the American Meteorological Society*, *98*, 163–173. https://doi.org/10.1175/BAMS-D-16-0017.1
Wanders, N. N., Bachas, A. A., He, X. G., Huang, H. H., Koppa, A. A., Mekonnen, Z. T., … Wood, E. F. (2017). Forecasting the hydroclimatic signature of the 2015/16 El Niño event on the Western United States. *Journal of Hydrometeorology*, *18*, 177–186. https://doi.org/10.1175/JHM-D-16-0230.1
Wang, S. Y., Hipps, L., Gillies, R. R., & Yoon, J.-H. (2014). Probable causes of the abnormal ridge accompanying the 2013–2014 California drought: ENSO precursor and anthropogenic warming footprint. *Geophysical Research Letters*, *41*, 3220–3226. https://doi.org/10.1002/2014GL059748
Wheeler, M. C., Zhu, H., Sobel, A. H., Hudson, D., & Vitart, F. (2016). Seamless precipitation prediction skill comparison between two global models. *Quarterly Journal of the Royal Meteorological Society*. https://doi.org/10.1002/QJ.2928
Xie, P., Yatagai, A., Chen, M., Hayasaka, T., Fukushima, Y., Liu, C., & Yang, S. (2007). A gauge-based analysis of daily precipitation over East Asia. *Journal of Hydrometeorology*, *8*, 607–626.
Zhu, H., Wheeler, M. C., Sobel, A. H., & Hudson, D. (2014). Seamless precipitation prediction skill in the tropics and extratropics from a global model. *Monthly Weather Review*, *142*, 1556–1569.